# Double-folding nucleus-nucleus potential based on the self-consistent calculations

1. Introduction
2. Nucleus-nucleus interaction potentials
3. EDF for nuclear ground-state density profiles
4. Useful parameterization
5. Coulomb barriers and sub-barrier fusion
6. Modification of Skyrme EDF
7. Summary

G.Adamian, N.Antonenko, V.Sargsyan, H.Lenske
A.Severyukhin, N.Arsenyev

-EDF and nuclear properties. The central density and radius are mainly related to the internal NN forces.

-The diffuseness of the nuclear surface is related to the external part of NN forces or to the effect of finite Fermi-system.

-Nucleus-nucleus potentials (hight and position of the Coulomb barrier).

-Sub-barrier fusion in astrophysical reactions.

Self-consistent approaches: relativistic and non-relativistic
Micro-macro models

RMF [J. Meng, H. Toki, S.G. Zhou, S.Q. Zhang, W.H. Long, and L.S. Geng, Prog. Part. Nucl. Phys. **57**, 470 (2006)]

The non-covariant EDFs. The fit of these EDFs involves binding energies, $Q_\alpha$-values in heavy and superheavy nuclei, and nuclear structure effects. The equilibrium deformations are determined by the minimization of the total energy of the system.
SV-bas [P. Klupfel, P.-G. Reinhard, T.J. Buervenich, and J.A. Maruhn, PRC **79**, 034310 (2009)]
Giessen EDF [F.Hofmann and H.Lenske, PRC 57, 2281 (1998)]

MM models [P.Möller *et al.*; A.Sobiczewski *et al.*; P.Jachimowicz, M.Kowal, and J.Skalski, At. Data Nucl. Data Tables **138**, 101393 (2021); Lublin model] provide stronger shell effects at $Z$ = 114 and $N$ = 184.
With the TCSM (like in the RMF and Skyrme self-consistent treatments) the proton shell closure is expected at $Z$ = 120-126 and there are strong shell effects at $N$ = 184.

The nucleus-nucleus interaction potential $V$ is represented as the sum

$$V(R) = V_C(R) + V_N(R) + V_R(R)$$

of the Coulomb, nuclear, and centrifugal potentials.

The double-folding procedure

$$V_N(R) = \int d\mathbf{r_1} d\mathbf{r_2}\, \rho_1(\mathbf{r_1})\rho_2(\mathbf{R} - \mathbf{r_2})F(\mathbf{r_2} - \mathbf{r_1}).$$

The effective $NN$ forces

$$F(\mathbf{r_2} - \mathbf{r_1}) = C_0\left(F_{in}x(\mathbf{r_1}) + F_{ex}\left(1 - x(\mathbf{r_1})\right)\right)\delta(\mathbf{r_2} - \mathbf{r_1}),$$

$$x(\mathbf{r_1}) = \rho_1(\mathbf{r_1}) + \rho_2(\mathbf{R} - \mathbf{r_2})$$

The Landau-Migdal parameters $F_{in}$ and $F_{ex}$, $C_0$ are determined from a fit to experimentally measured properties of nuclei

$$F = \frac{\delta^2 \mathcal{E}_{int}(x)}{\delta x^2} = C_0[F_{ex} + (F_{in} - F_{ex})x] \qquad \text{the Giessen EDF}$$

$$C_0 = 308 \text{ MeV}/\text{fm}^3 \quad \rho_0 = 0.16 \text{ fm}^{-3} \quad F_{ex} = -3.84 \quad F_{in} = 0.09$$

With a radial-dependent effective mass $m_q^*$ the equation for the single-particle wave function is as follows

$$\left(-\boldsymbol{\nabla}\cdot\frac{\hbar^2}{2m_q^*(\mathbf{r})}\boldsymbol{\nabla}+V_q(\mathbf{r})+V_q^{(ls)}(\mathbf{r})-\varepsilon_q\right)\psi_q(\mathbf{r})=0.$$

The self-consistent approaches lead to single-particle potentials given in non-relativistic formulation by

$$U_q(\rho)=V_q(\rho)+V_q^{(ls)}(\rho)=\frac{\hbar^2k_{\mathrm{F}_q}^2}{2m_q}\left(1-\frac{m_q}{m_q^*}\right)+\Sigma_q(k_{\mathrm{F}_q},\rho)+V_q^{(ls)}(\rho)$$

$\Sigma_q(k,\rho)$ - self-energies, $k_{\mathrm{F}_q}$ - wave number at the Fermi surface, $m_q$ – bare nucleon mass. Reduction to the standard Schrödinger equation [EPJA 54, 170 (2018); 57, 89 (2021)]

$$\left(-\frac{\hbar^2}{2m_q}\boldsymbol{\nabla}^2+U_q(r)+U_q^{(ls)}(r)-\varepsilon_q\right)\psi_q(r)=0,$$

$$U_q(r)=V_q(r)+\frac{\hbar^2}{2m_q}\mu_q(r)\bar{k}_{\mathrm{eff}}+\frac{3}{5}\left(1-\frac{m_q^*(r)}{m_q}\right)\frac{\hbar^2k_{\mathrm{F}_q}^2(r)}{2m_q^*(r)}$$

$$U_q^{(ls)}(r)=\frac{m_q^*(r)}{m_q}V_q^{(ls)}(r)=-\frac{1}{m_q}\frac{1}{r}\frac{\mathrm{d}\ln(m_q^*(r)/m_q)}{\mathrm{d}r}\mathbf{l}\cdot\mathbf{s}$$

# Giessen EDF for nuclear ground-state density profiles

Nuclear binding energies, single-particle states, and ground-state densities are described by an energy density functional

$$\mathcal{E}(\rho_q, \tau_q, \kappa_q) = \mathcal{E}_{kin}(\tau_q) + \frac{1}{2}\mathcal{E}_{int}(\rho_q) + \frac{1}{2}\mathcal{E}_{pair}(\rho_q, \kappa_q) - \sum_{q=p,n} \lambda_q \rho_q$$

The proton (q = p) and neutron (q = n) densities

$$\rho_q = \sum_{jm} v_{jm}^2 |\varphi_{qjm}|^2,$$

corresponding kinetic energy densities

$$\tau_q = \sum_{jm} v_{jm}^2 \frac{\hbar^2}{2m_q} |\nabla \varphi_{qjm}|^2,$$

and pairing densities,

$$\kappa_q = \frac{1}{2} \sum_{jm} u_{jm} v_{jm} |\varphi_{qjm}|^2.$$

# Nucleon density distribution

The nucleon density distribution in the spherical nucleus is usually taken in the three-parameter symmetrized Fermi-type form

$$\rho(r) = \frac{\rho_0}{1 + \exp[(r - R)/a]},$$

where $\rho_0$ is the saturated nucleon density in the center of nucleus, $R = r_0 A^{1/3}$ is the nuclear radius with the parameter $r_0$, and $a$ is the nuclear diffuseness.

The value of

$$\rho_0 = \frac{3}{4\pi r_0^3} \frac{1}{1 + \left(\frac{\pi a}{r_0 A^{1/3}}\right)^2},$$

provides the proper normalization. Two-parameter fit of the nuclear density profile provides $r_0$= 1.073 and 1.081 fm, $a$=0.538 and 0.53 fm for $^{40}Ca$ and $^{48}Ca$, respectively.

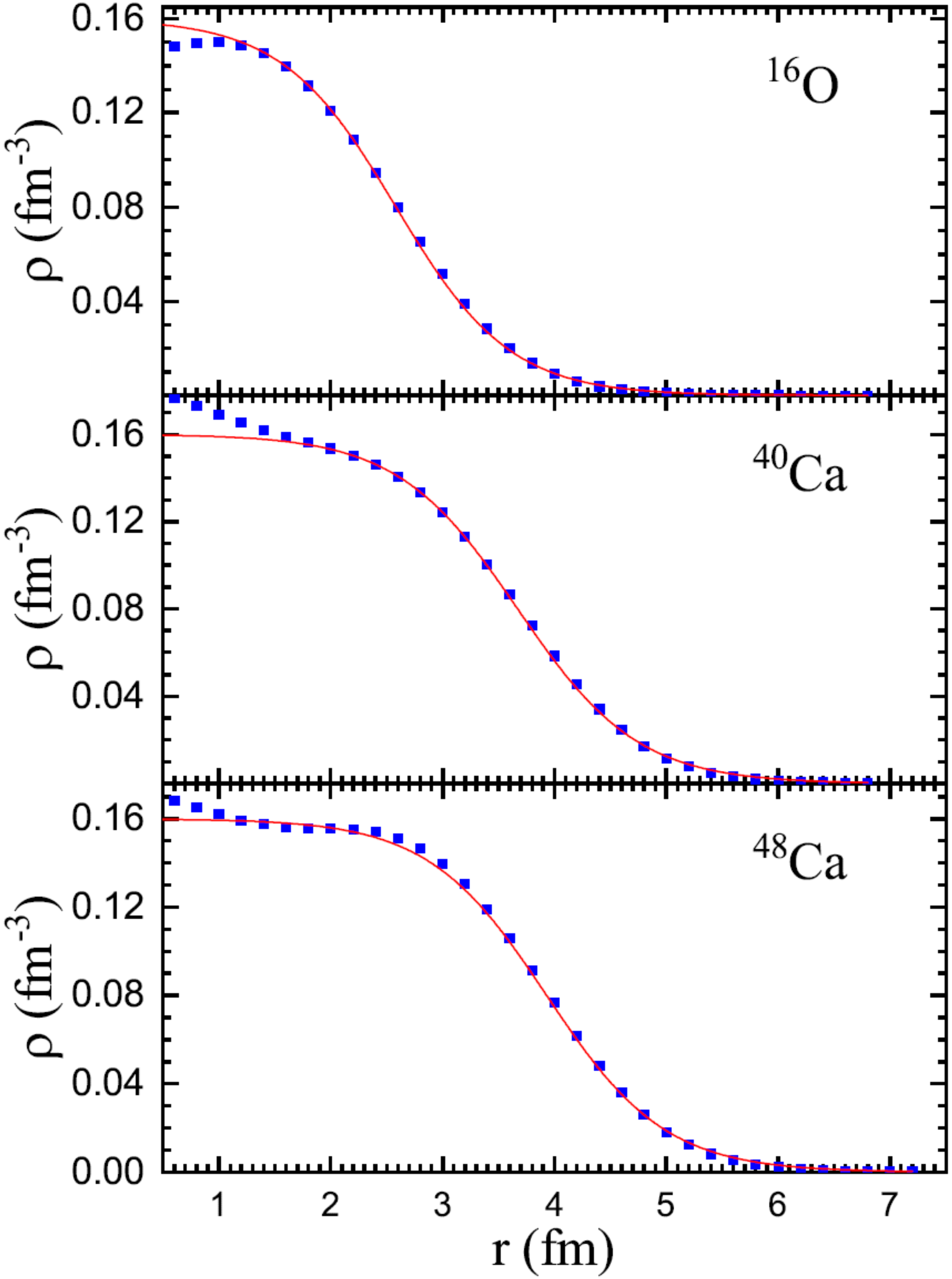


Self-consistent HFB nucleon-density distributions (symbols) in indicated spherical nuclei are fitted by the Fermi-type form where always $\rho_0$ = 0.16 fm$^{-3}$ (lines).

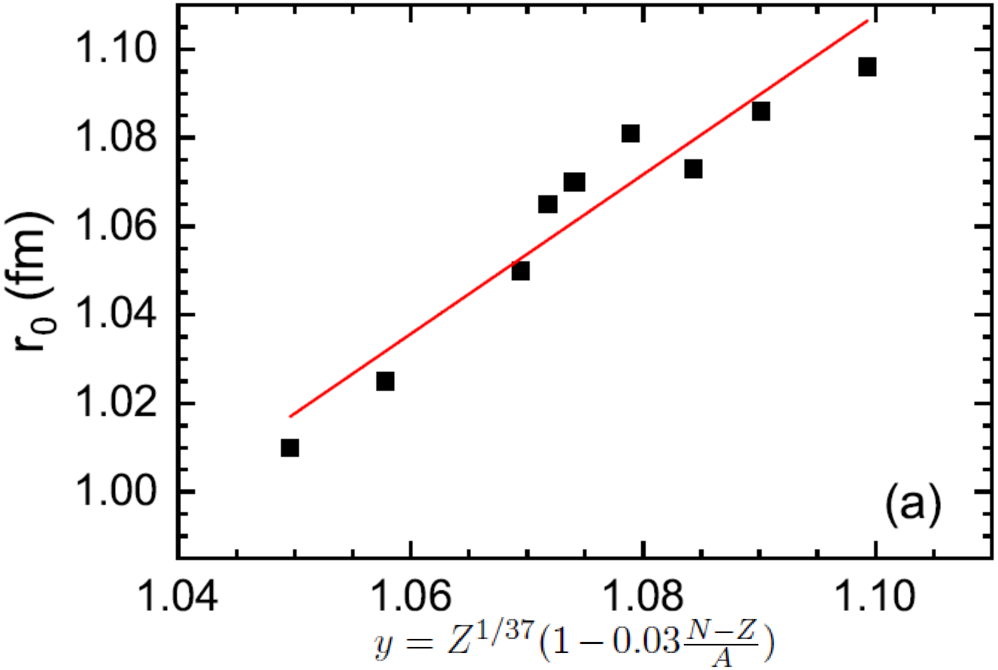


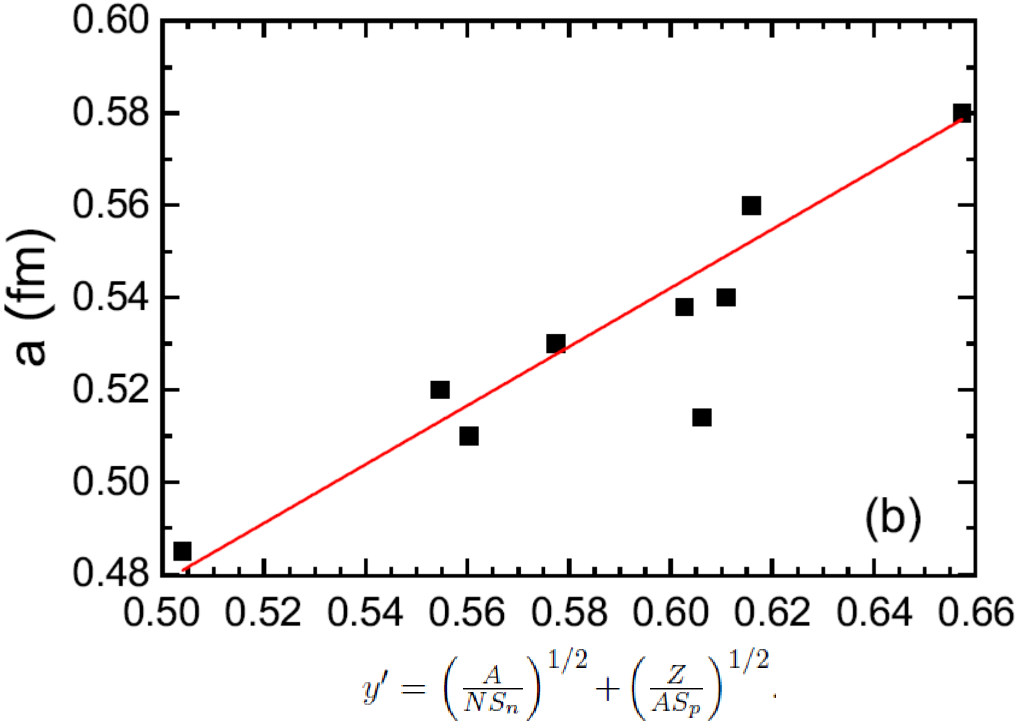


# Useful parameterizations

$$r_0 = 1.8Z^{1/37}\left(1 - 0.03\frac{N-Z}{A}\right) - 0.87 \text{ [fm]},$$

$$a = 0.64\left[\left(\frac{A}{NS_n}\right)^{1/2} + \left(\frac{Z}{AS_p}\right)^{1/2}\right] + 0.16 \text{ [fm]}$$

# PARAMETERIZATION OF THE NUCLEAR PART OF NUCLEUS-NUCLEUS INTERACTION POTENTIAL

For spherical nuclei, the nuclear part of nucleus-nucleus interaction potential can be parameterized by the Morse-type potential

$$V_N(R) = D\left[\exp\left(-2\frac{R-R_0'}{d}\right) - 2\exp\left(-\frac{R-R_0'}{d}\right)\right].$$

A good description of the heights of the Coulomb barriers is achieved at

$$\begin{aligned} D &= 49.3\frac{R_{01}R_{02}}{R_{01}+R_{02}}\sqrt{\frac{a_1a_2}{a_1+a_2}}, && \text{[MeV]} \\ R_0' &= 0.98(R_{01}+R_{02})\sqrt{a_1+a_2}, && \text{[fm]} \\ d &= 0.8\sqrt{a_1+a_2}, && \text{[fm]} \end{aligned}$$

# Coulomb barriers and sub-barrier fusion

TABLE I: The calculated values of $V_b$, $R_b$, and $\omega_b = \sqrt{\frac{1}{\mu}\frac{d^2V(R)}{dR^2}|_{R=R_b}}$ are compared with those for phenomenologically adjusted potentials in Ref. [23]. The nuclei are assumed to be spherical.

| Reaction | $R_b$ (fm) | | $V_b$ (MeV) | | $\omega_b$ (MeV) | |
|---|---|---|---|---|---|---|
| | [23] | calc | [23] | calc | [23] | calc |
| $^{12}$C + $^{12}$C | 7.95 | 8.06 | 6.00 | 5.94 | 2.67 | 2.70 |
| $^{12}$C + $^{16}$O | 8.32 | 8.32 | 7.64 | 7.67 | 2.68 | 2.77 |
| $^{12}$C + $^{30}$Si | 8.71 | 8.79 | 12.81 | 12.75 | 3.00 | 3.07 |
| $^{16}$O + $^{16}$O | 8.69 | 8.57 | 9.75 | 9.94 | 2.67 | 2.82 |
| $^{28}$Si + $^{28}$Si | 9.08 | 9.05 | 28.64 | 28.95 | 3.27 | 3.50 |
| $^{28}$Si + $^{30}$Si | 9.28 | 9.27 | 28.07 | 28.27 | 3.16 | 3.33 |
| $^{30}$Si + $^{30}$Si | 9.45 | 9.49 | 27.52 | 27.32 | 3.04 | 3.16 |
| $^{24}$Mg + $^{30}$Si | 9.28 | 9.31 | 24.07 | 24.09 | 3.06 | 3.16 |
| $^{40}$Ca + $^{40}$Ca | 10.08 | 9.99 | 52.46 | 53.34 | 3.22 | 3.47 |
| $^{48}$Ca + $^{48}$Ca | 10.58 | 10.59 | 50.46 | 50.69 | 2.95 | 3.08 |
| $^{36}$S + $^{48}$Ca | 10.34 | 10.29 | 41.20 | 41.65 | 2.90 | 3.09 |
| $^{36}$S + $^{64}$Ni | 10.70 | 10.62 | 55.68 | 56.45 | 3.03 | 3.24 |

[23] Physics Letters B 824 (2022) 136792

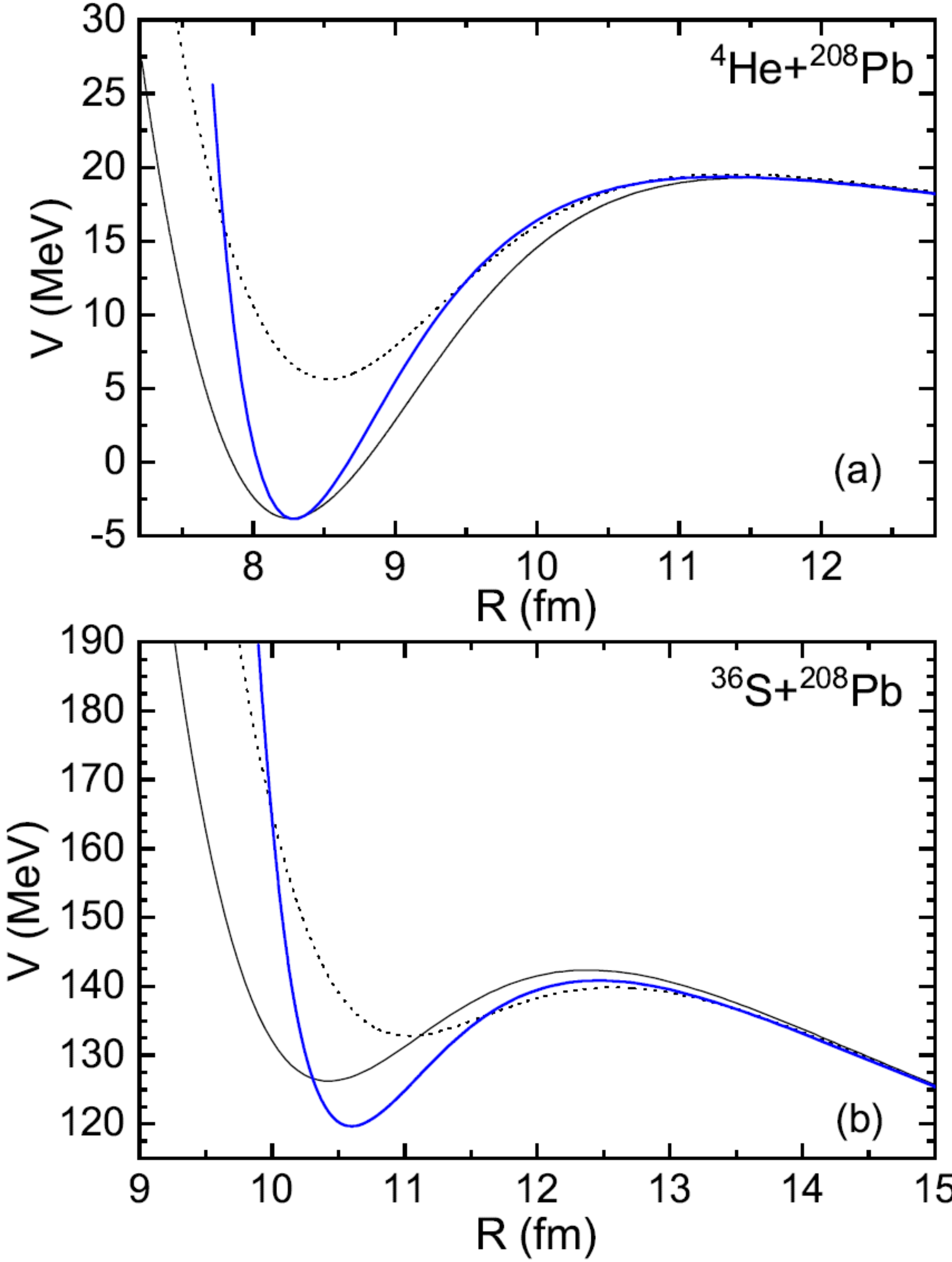


Comparison of nucleus-nucleus interaction potentials calculated with self-consistent (solid lines) and phenomenological (dashed lines) [23] nucleon densities for the reactions $^{4}$He+$^{208}$Pb (a) and $^{36}$S+$^{208}$Pb (b). The results of calculation with the parametrization of the nuclear part of the potential are shown by blue lines.

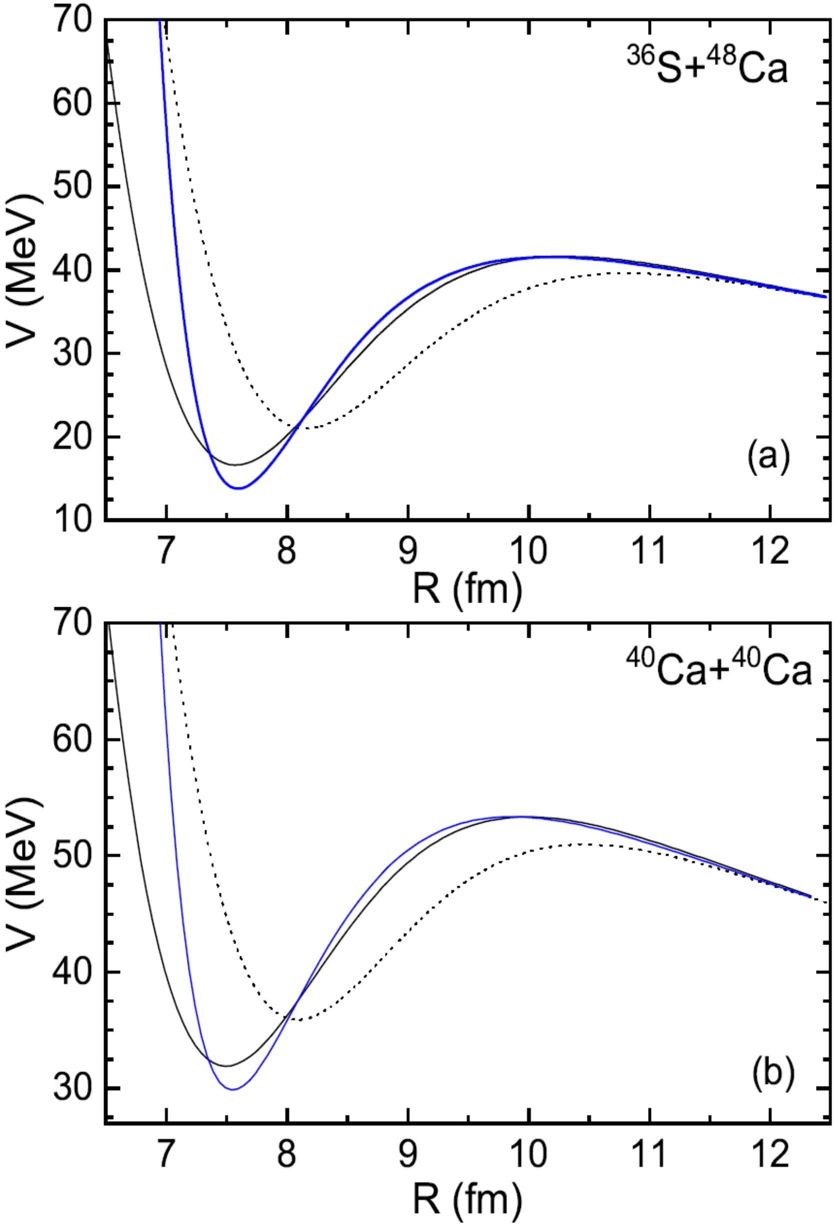

$^{36}S+^{48}Ca$
(a)
V (MeV)
R (fm)
$^{40}Ca+^{40}Ca$
(b)
V (MeV)
R (fm)


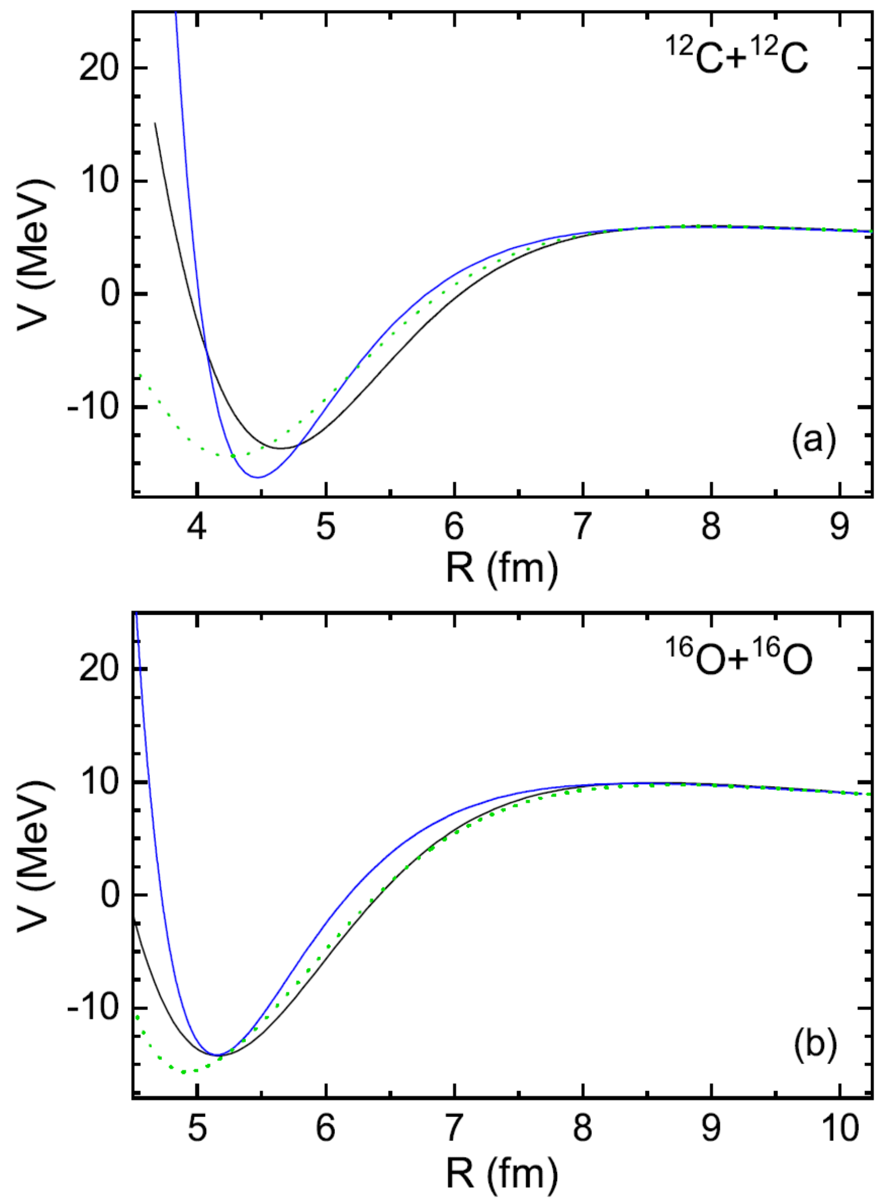

$^{12}C+^{12}C$
(a)
V (MeV)
R (fm)
$^{16}O+^{16}O$
(b)
V (MeV)
R (fm)

For low-energy reactions with light- and medium-mass nuclei, the fusion cross section at the given center-of-mass energy $E_{\mathrm{c.m.}}$ is written as a sum over partial waves $l$

$$\sigma(E_{\mathrm{c.m.}}) = \frac{\pi\hbar^2}{2\mu E_{\mathrm{c.m.}}} \sum_l (2l+1)\bar{P}_l(E_{\mathrm{c.m.}}),$$

$$\bar{P}_l = \int_0^{\pi/2}\int_0^{\pi/2} d\cos\theta_1 \, d\cos\theta_2 \, P_l(E_{\mathrm{c.m.}},\theta_1,\theta_2),$$

$$P_l = \frac{1}{2}\mathrm{erfc}\left[\sqrt{\frac{\pi(V_b - E_{\mathrm{c.m.}})}{\kappa\hbar\omega}}\right], \qquad \kappa = \sqrt{\frac{2V_b}{\mu\omega_b^2(R_1+R_2)^2 - 2V_b}}.$$

$$\omega = \left(\frac{2[V_b - E_{\mathrm{c.m.}}]}{\mu[R_{\mathrm{ext}} - R_b]^2}\right)^{1/2},$$

$R_{ext}$, $R_b$ and $V_b$ are the external turning point, the position and height of the Coulomb barrier, respectively.

Physics Letters B 824 (2022) 136792

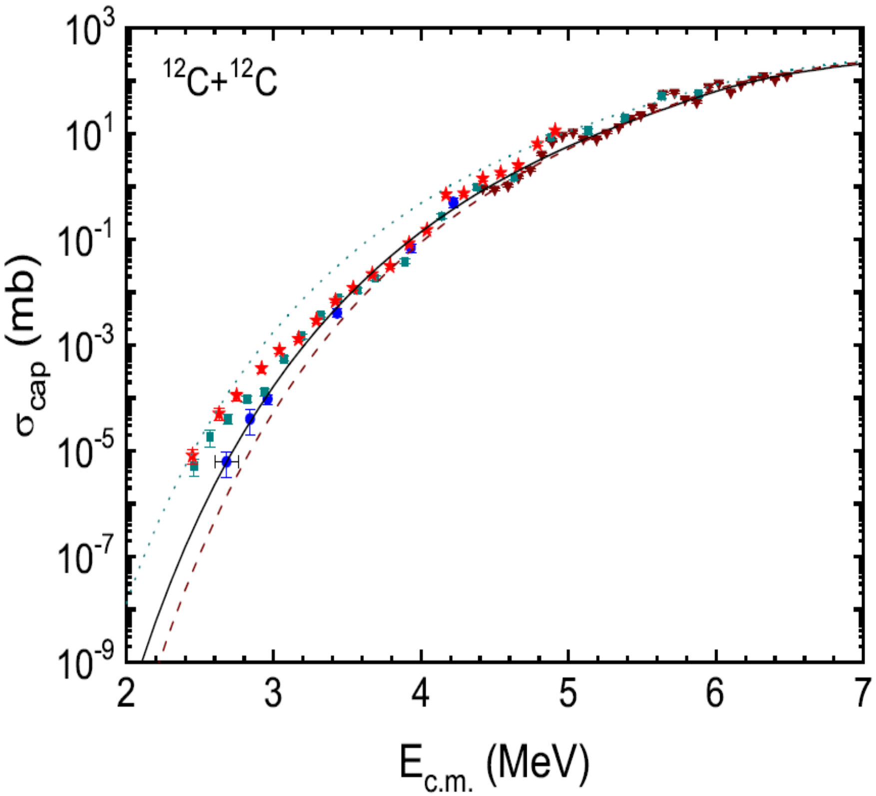


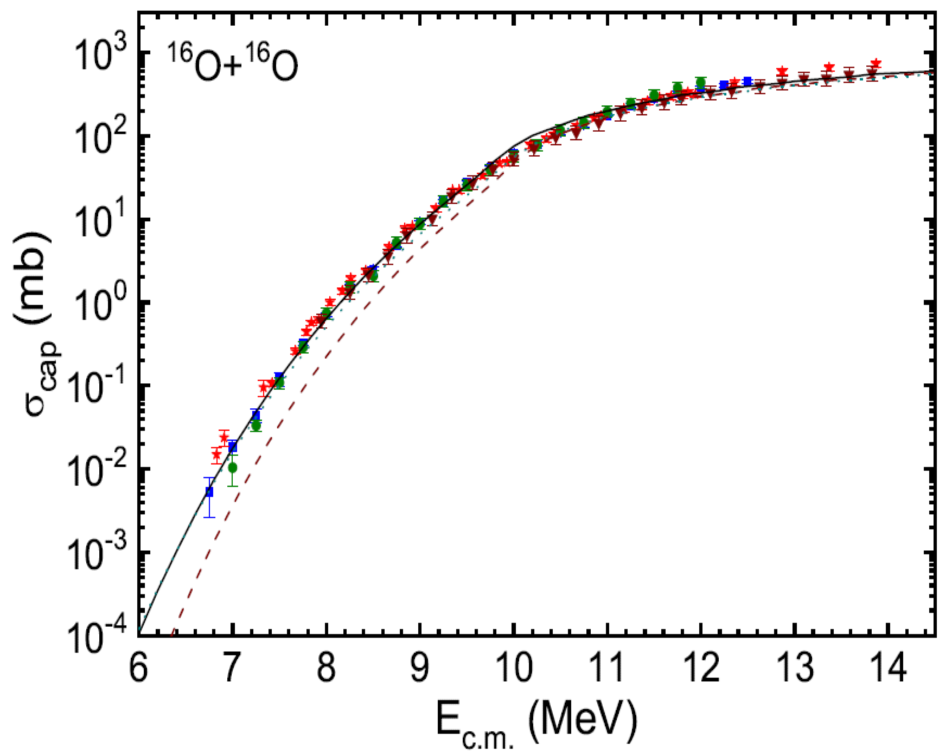


The fusion excitation functions calculated with phenomenologically adjusted (*solid lines*), self-consistent (*dashed line*), and parameterized (*dotted line*) potentials for the $^{12}$C+ $^{12}$C reaction. The experimental data are taken from [PRC 97, 012801(R) (2018)] (blue symbols), [PRC 73, 064601 (2006)] (black symbols), [PRL 124, 192701 (2020)] (red symbols), [PRL 124, 192702 (2020)] (wine symbols), [PRL 98, 122501 (2007)] (green symbols).

The experimental data are taken from [PRC 31, 1980 (1985)] (black symbols), [Z. Phys. A297, 161 (1980)] (blue symbols), [NPA 422, 373 (1984)] (red symbols) and [PRC 35, 591 (1987)] (wine symbols).

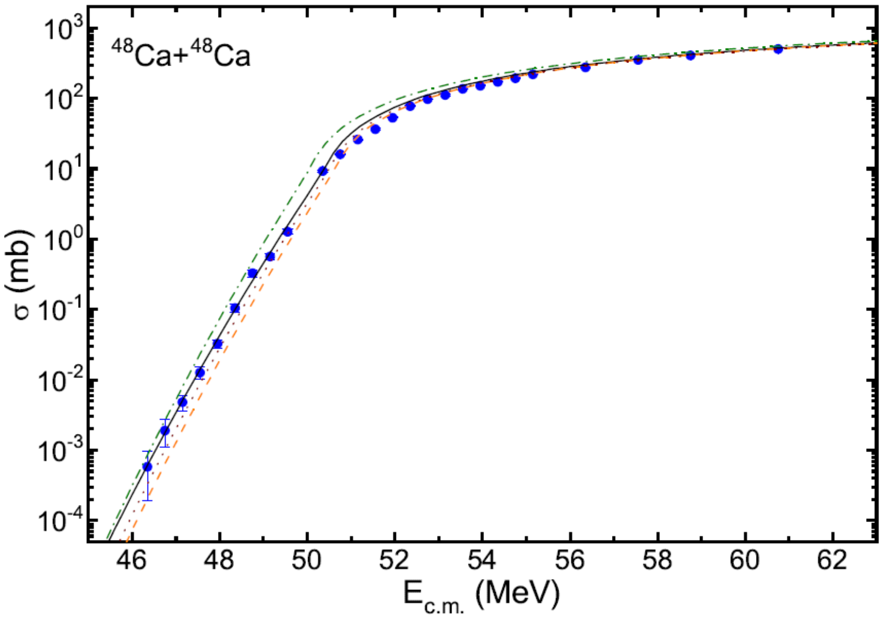


The experimental data are taken from [PLB 679, 95 (2009)] (symbols). The cross sections calculated with the self-consistent nucleus-nucleus potential obtained with $F_{ex}$ = - 4.484 are shown by dash-dotted line.

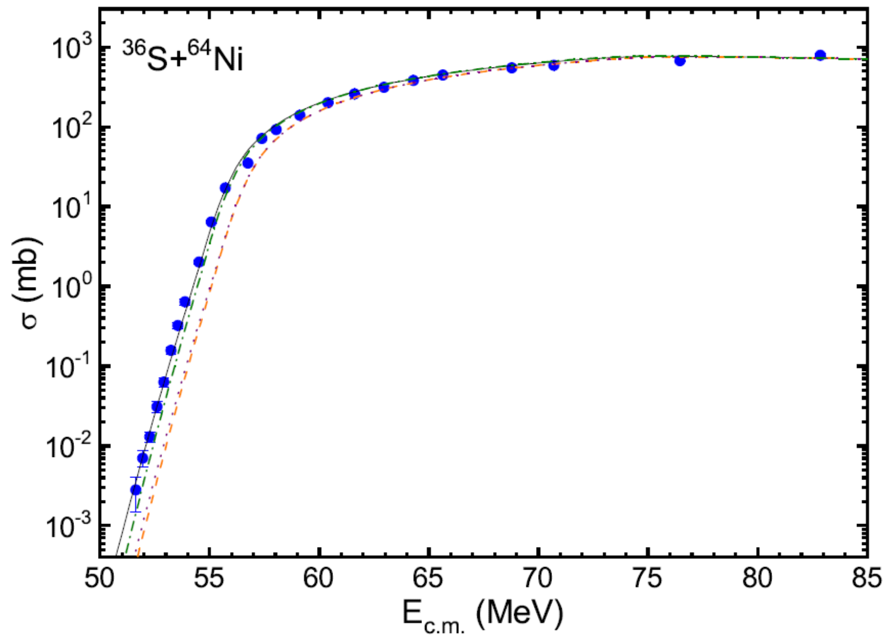


The experimental data are taken from [PRC 82, 064609 (2010)] (symbols). The cross sections calculated with the self-consistent nucleus-nucleus potential obtained with $F_{ex}$ = - 4.484 are shown by dash-dotted line.

# Modification of Skyrme EDF

$$\langle \Psi | H | \Psi \rangle = \int \mathcal{H}(\boldsymbol{r})\, d^3 r ,$$

with:

$$\mathcal{H} = \mathcal{K} + \mathcal{H}_0 + \mathcal{H}_3 + \mathcal{H}_{\text{eff}} + \mathcal{H}_{\text{fin}} + \mathcal{H}_{\text{so}} + \mathcal{H}_{\text{sg}} + \mathcal{H}_{\text{Coul}} ,$$

where $\mathcal{K} = \frac{\hbar^2}{2m}\tau$ is the kinetic-energy term, $\mathcal{H}_0$ a zero-range term, $\mathcal{H}_3$ the density-dependent term, $\mathcal{H}_{\text{eff}}$ an effective-mass term, $\mathcal{H}_{\text{fin}}$ a finite-range term, $\mathcal{H}_{\text{so}}$ a spin–orbit term and $\mathcal{H}_{\text{sg}}$ a term due to the tensor coupling with spin and gradient.

$$\mathcal{H}_0 = \frac{1}{4} t_0 \left[ (2 + x_0)\, \rho^2 - (2x_0 + 1) \left( \rho_{\text{p}}^2 + \rho_{\text{n}}^2 \right) \right] ,$$

$$\mathcal{H}_3 = \frac{1}{24} t_3 \rho^{\sigma} \left[ (2 + x_3)\, \rho^2 - (2x_3 + 1) \left( \rho_{\text{p}}^2 + \rho_{\text{n}}^2 \right) \right] ,$$

$$\mathcal{H}_{\text{eff}} = \frac{1}{8} \left[ t_1 (2 + x_1) + t_2 (2 + x_2) \right] \tau \rho + \frac{1}{8} \left[ t_2 (2x_2 + 1) - t_1 (2x_1 + 1) \right] \left( \tau_{\text{p}} \rho_{\text{p}} + \tau_{\text{n}} \rho_{\text{n}} \right) ,$$

$$\mathcal{H}_{\text{fin}} = \frac{1}{32} \left[ 3t_1 (2 + x_1) - t_2 (2 + x_2) \right] (\boldsymbol{\nabla} \rho)^2 - \frac{1}{32} \left[ 3t_1 (2x_1 + 1) + t_2 (2x_2 + 1) \right] \left[ (\boldsymbol{\nabla} \rho_{\text{p}})^2 + (\boldsymbol{\nabla} \rho_{\text{n}})^2 \right] ,$$

$$\mathcal{H}_{\text{so}} = \frac{1}{2} W_0 \left[ \boldsymbol{J} \cdot \boldsymbol{\nabla} \rho + \boldsymbol{J}_{\text{p}} \cdot \boldsymbol{\nabla} \rho_{\text{p}} + \boldsymbol{J}_{\text{n}} \cdot \boldsymbol{\nabla} \rho_{\text{n}} \right] ,$$

$$\mathcal{H}_{\text{sg}} = -\frac{1}{16} (t_1 x_1 + t_2 x_2)\, \boldsymbol{J}^2 + \frac{1}{16} (t_1 - t_2) \left[ \boldsymbol{J}_{\text{p}}^2 + \boldsymbol{J}_{\text{n}}^2 \right] .$$

Total densities are defined as $\rho = \rho_{\text{p}} + \rho_{\text{n}}$, $\tau = \tau_{\text{p}} + \tau_{\text{n}}$, $J = J_{\text{n}} + J_{\text{p}}$.

# Summary

- If the neutron shell closure appears at a level with large orbital momentum, the nuclear diffuseness decreases.

- The non-covariant SC approach provides a good description of fusion reactions with light nuclei. Without adjusting parameters, there is a good description of sub-barrier fusion.

- EDF for the SC calculation of the Coulomb barriers